Chemical Science

Accepted Manuscript

This article can be cited before page numbers have been issued, to do this please use: Z. Fan, W. Fang, Y. Liu, Z. Xiao, J. Yu, X. He, X. Wang, X. Tang, L. Xia, L. Tang and T. He, *Chem. Sci.*, 2025, DOI: 10.1039/D5SC04010H.

ROYAL SOCIETY OF CHEMISTRY

rsc.li/chemical-science

View Article Online
DOI: 10.1039/D5SC04010H

ARTICLE

Sunlight-driven Photoinduced Electron/Energy Transfer-Reversible Addition-Fragmentation Chain Transfer Polymerization at Large Scale

Received 00th January 20xx,
Accepted 00th January 20xx

DOI: 10.1039/x0xx00000x

Zi-Hui Fan,[†a] Wei-Wei Fang,[†b,a] Yi-Xing Liu,[a] Zheng-Hao Xiao,[c] Jian-Kun Yu,[a] Xu-Yi He,[d] Xian-Zhen Wang,[a] Xue-Ning Tang,[e] Lei Xia,*[a] Long-Xiang Tang,*[a] Tao He*[a]

Abstract: Photoinduced electron/energy transfer-reversible addition-fragmentation chain transfer (PET-RAFT) polymerization is a sustainable and powerful tool to synthesize polymers and copolymers. However, development of large-scale production and polymerizations using sunlight irradiation remain top challenges for PET-RAFT polymerizations. In this study, conjugated cross-linked phosphine (PPh_3-CHCP) was explored as heterogeneous photocatalyst for efficient PET-RAFT polymerization. This development allowed PET-RAFTs to achieve high monomer conversions, low dispersity and good chain-end fidelity under a broad range of wavelengths and sunlight irradiation from various monomers. The heterogeneous PPh_3-CHCP photocatalyst could be easily separated and reused without an obvious structural deterioration and decrease in efficiency. Sunlight-driven photopolymerization of MA (methyl acrylate) was scaled up to 2 L (conversion 93%), and the obtained polymer showed good control over both molecular weight and dispersity ($Đ$= 1.13). White light driven polymerization of MA (conversion 91%, $Đ$ = 1.27) reached 6 L scale. These results demonstrate the great potential for industrial applications.

Introduction

Reversible-deactivation radical polymerizations (RDRPs) have emerged as a versatile and useful method to prepare well-defined polymeric materials.[1,2] Recently, consistent efforts have been made to employ light as energy source for RDRPs, as it allowed spatiotemporal control over polymerization, and provided an alternative avenue for polymers synthesis through green and sustainable processes.[3,4] In these polymerizations, photocatalysts converted photon energy into chemical energy and triggered the generation of propagating radicals, which played a critical role. Up to present, various photocatalysts and related photo-RDRPs have been developed, such as photocatalyzed atom transfer radical polymerization (photo-ATRP) and photoinduced electron/energy transfer-reversible addition-fragmentation chain transfer (PET-RAFT) polymerizations, etc.[5-9] Compared with photo-ATRP especially photoinduced metal-catalyzed ATRP, PET-RAFT don't need to use or only applied tiny amount of toxic metal complex,[10,11] which make the purification of obtained polymers much easier and more convenient to be applied in industrials.

In recent PET-RAFT studies, great progress has been made in enhancing polymerization efficiency and versatility.[12,13] However, although it is highly desired by industrials, there is relatively slow progress in developing large scale PET-RAFT due to typical barriers. For example, the light intensity needs to be greatly increased to overcome the adverse effects which are derived from the light absorption of reactants or light scattering of heterogenous photocatalyst at large-scale synthesis.[14] It was reported that the combination with flow devices offered an opportunity to develop scale-up PET-RAFT, as the high surface-area-to-volume of photoreactor were beneficial to mass transfer and light penetration.[15] However, negative features such as deviation of prepared polymers and undesired side reactions were observed, especially when extending the reactor length, residence time, or raising the monomer concentration.[16,17] Up to present, the scale of most PET-RAFTs are below 200 mL.[18,19]

Sunlight is an inherently abundant high-intensity light source, and sunlight-driven polymerizations are undoubtedly valuable for green and sustainable scale-up production. However, successful sunlight-driven PET-RAFT is very challenging. One of the typical reasons is that the high illumination intensity of sunlight (higher than 1000 W m^{-2}) may result in the irreversible deterioration of the excited

[a.] School of Chemistry and Chemical Engineering, Anhui Province Key Laboratory of Value-Added Catalytic Conversion and Reaction Engineering, Anhui Province Engineering Research Center of Flexible and Intelligent Material, Hefei University of Technology, Hefei, Anhui 230009, P. R. China
E-mail: lxia@hfut.edu.cn, tanglx@hfut.edu.cn, taohe@hfut.edu.cn
[b.] School of Chemistry and Chemical Engineering, Key Laboratory of Material Chemistry for Energy Conversion and Storage Ministry of Education, Hubei Key Laboratory of Material Chemistry and Service Failure, Huazhong University of Science and Technology, Wuhan, Hubei 430074, P. R. China
[c.] School of Microelectronics, Microelectronics Science and Engineering, Southern University of Science and Technology, Shenzhen, Guangdong 518005, P. R. China
[d.] University of Science and Technology of China, Hefei, Anhui 230026, P. R. China
[e.] School of Data Science, The Chinese University of Hong Kong, Shenzhen, Shenzhen, Guangdong 518172, P.R. China
† Z. H. F and W. W. F contributed equally to this work.
Supplementary Information available: [details of any supplementary information available should be included here]. See DOI: 10.1039/x0xx00000x

View Article Online DOI: 10.1039/D5SC04910H

molecules.[20-22] Meanwhile, the high-energy photons in the solar spectrum could also lead to undesirable side reactions (eg. self-initiation of monomers and degradation of polymers containing unstable groups in main chains). As a result, the scale of most sunlight driven PET-RAFTs was less than 3 mL. The photocatalysts applied in present PET-RAFTs mainly covered homogeneous (eg. dyes and related compounds, organocatalysts, etc.)[23-27] and heterogenous (eg. bioactive,[28] nanoparticles (NPs),[29-32] metal organic frameworks (MOFs),[33-35] covalent organic frameworks (COFs),[36,37] carbon-based nanomaterials,[38-40] nanocomposites[41,22]) materials. Whereas heterogeneous photocatalysts arouse widespread interest for their facile recycling, minimal catalyst requirements (eg, EY-SNP, 3 ppm),[43] excellent tolerance to oxygen, etc. Although these photocatalysts could be applied in polymerizations under different light irradiations (eg. UV (ultraviolet), blue, green, red, NIR (near infra-red) and white), potential photobleaching makes most molecular photocatalysts lack the capability of long-term operation under sunlight irradiation. Meanwhile, for most of the photocatalysts utilized in sunlight-driven photopolymerizations, it was challenging to achieve ideal monomer conversions (eg. >90%) within a short period (eg. 6-8 hours).[41,44] Although carbon nanodots (CDs) and Ag_2S nanocrystals could offer polymers with high conversions and well-controlled molecular weights, the purification was relatively complicated due to their nano-scale size.[31,38] Other heterogenous photocatalysts such as Ag_3PO_4 NPs and zirconium-porphyrin frameworks (ZrPHPs) could facilitate nearly quantitative monomer conversions, but they were subjected to relatively broad dispersity of the synthesized polymers or narrow choice of monomers.[29,35]

Ideally, photocatalyst applied in large scale sunlight-driven PET-RAFT should have a high absorption coefficient in visible and NIR range, in order to enhance photon penetration and avoid competitive absorption of reactant. The photocatalyst should also have suitable redox potential to reduce chain transfer agent and regulate the reversible deactivation process. Although great progress has been made in PET-RAFT recently, the development of stable materials and efficient methodology to employ sunlight directly at large scale synthesis with good control over the polymer's molecular weight and dispersity has remained a big challenge. This is clearly an area worth exploring, keeping in view the potential for practical industrial applications, together with the green and sustainable nature.

π-conjugation extension as well as the introduction of halogens were the most applied guiding principles for designing long-wavelength absorbing photocatalyst.[45] Additionally, benefiting from the extended conjugated network which provides a pristine site for carrier transport, heterogeneous photocatalysts (eg. TPP-ImBr-CPP,[46] TAPPY-DTDD-CMP,[47] TCPP-TPDA-COF[48]) showed enhanced electron transfer capability under light irradiation, which offered a robust platform for the development of PET-RAFT polymerization. Previously, we reported the synthesis and applications of PPh_3-CHCP in photo-ATRP.[49] With the deep understanding of the PET-RAFT polymerization mechanism and continuous investigation on rational design of photocatalyst, herein, we think that PPh_3-CHCP, being constructed by crosslinked phosphine and substituted aromatic group (Fig. S1†), may serve as an efficient photocatalyst for PET-RAFT. This is because that it showed moderate photocatalytic activity under visible light irradiation. In this work, PPh_3-CHCP was served as photocatalyst for PET-RAFT polymerization, achieving high monomer conversion and controllable molecular weight properties under varying light irradiation including sunlight. The heterogeneous nature of PPh_3-CHCP enables it to maintain photocatalytic performance after multiple recycling processes. White light driven polymerization of MA (methyl acrylate) (conversion 91%, $Đ$ = 1.27) reached 6L scale. In addition, sunlight-induced PET-RAFT could be successfully conducted at 2 L scale (Fig. 1a), which produced PMA with 93% conversion and good control over dispersity ($Đ$ = 1.13), demonstrating its great potential for industrial applications.

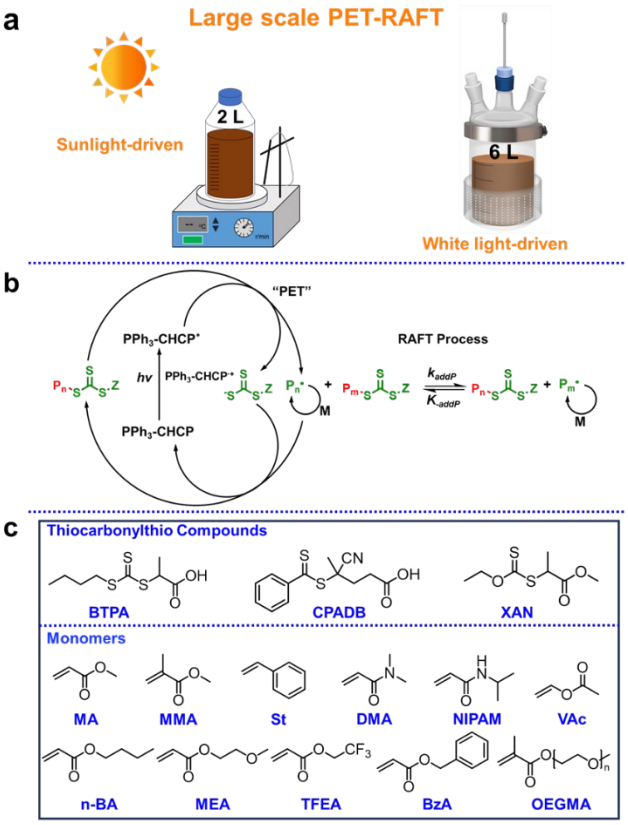

Fig. 1 Development of photocatalyst for large scale PET-RAFT. (a) Large scale PPh_3-CHCP-catalyzed PET-RAFT polymerization (2 L reaction scale of PMA under sunlight irradiation and 6 L reaction scale of PMA under white light irradiation). (b) Mechanism of PPh_3-CHCP-catalyzed PET-RAFT polymerization. (c) List of RAFT agents and monomers investigated in this study. MA (Methyl acrylate), MEA ((2-methoxyethyl) acrylate), BzA (benzyl acrylate), n-BA (n-butyl acrylate), TFEA (2,2,2-trifluoroethyl acrylate), MMA (methyl methacrylate), OEGMA (poly (ethylene glycol) methyl ether methacrylate), NIPAM (N-isopropylacrylamide), DMA (N,N-dimethylacrylamide), St (styrene), and VAc (vinyl acetate). BTPA (2-(((butylthio)carbonothioyl)thio)propanoic acid), CPADB (4-cyano-4-(phenylcarbonothioylthio)pentanoic Acid). XAN (2-(Ethoxythioxomethylthio)propionic acid methyl ester).

Results and discussion

PPh_3-CHCP catalyzed PET-RAFT polymerizations under blue light irradiation

The typical characterizations of PPh_3-CHCP photocatalyst were consistent with our previous report, indicating the successful construction (Fig. S2-S9†). Further cyclic voltammetry investigation of PPh_3-CHCP exhibited reduction potential of (E_{ox}^* = -1.35 V) (Fig. S10†), indicating that excited states of PPh_3-CHCP were highly reducing to reduce BTPA (2-(((butylthio)carbonothiolyl)thio)propanoic acid) (E_{red} = −0.6 V) and CPADB (4-cyano-4-(phenylcarbonothioylthio) pentanoic acid) (E_{red} = −0.4 V).[50]

The photocatalytic performance of PET-RAFT polymerization using PPh_3-CHCP were first evaluated under blue light irradiation (λ_{max} = 465 nm, 2 mW/cm^2), with MA as modal monomer and BTPA as CTA (chain transfer agent) (Fig. S11-12†). Polymerization of deoxygenated MA (freeze-pump-thaw) achieved 97% monomer conversion within 9 hours (Table 1, entry 3), and the molecular weight of PMA (M_n = 17000, $Đ$ = 1.07) was close to the theoretical value, indicating the good control of the polymerization. Applying nitrogen bubbling instead of freeze-pump-thaw as prior deoxygenation process could achieve similar results (Table S1†), which might be beneficial for potential industrial applications.

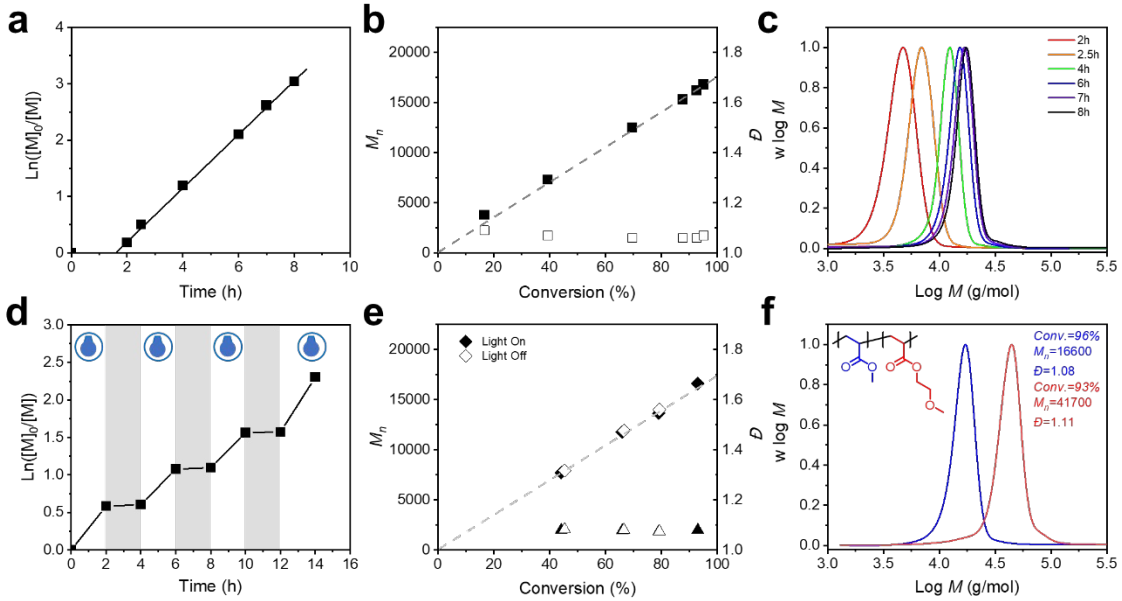

Fig. 2 Results for the polymerization of MA using PPh_3-CHCP photocatalyst. (a) Kinetics and (b) evolution of molecular weight (M_n, filled points) and dispersity ($Đ$, empty points) as a function of monomer conversion in PET-RAFT polymerization of MA. (c) SEC traces of PMA synthesized in the kinetic study. (d) "ON/OFF" experiments catalyzed by PPh_3-CHCP under blue LED irradiation. (e) Plot of M_n and $Đ$ (solid symbols indicate after irradiation, and open symbols indicate after dark period) versus monomer conversions in "ON/OFF" experiments. (f) SEC traces of PMA and PMA_{200}-*b*-$PMEA_{200}$ block copolymer synthesized by *in situ* chain extension.

The results of kinetic study were shown in Fig. 2. A linear dependence of $\ln([M]_0/[M]_t)$ with the exposure time corresponds to a pseudo first-order polymerization kinetics (Fig. 2a), suggesting a constant concentration of propagating radicals in the polymerization systems. PPh_3-CHCP in DMSO exhibited an induction period (<2 h), which might be due to the presence of dissolved trace amount of oxygen in the reaction solutions.[38] The experimental molecular weight (MW) values increased linearly with monomer conversion, which were in good agreement with the theoretical values. In addition, the dispersity decreased as the monomer conversion increased, and a narrow MW distribution ($Đ$ < 1.09) was finally obtained (Fig. 2b), corresponding to a controlled radical polymerization nature. Under blue light irradiation (2 mW/cm^2), an apparent polymerization rate constant (k_{app}) of 0.47 h^{-1} was observed. The $k_{p,app}$ for polymerization of MA using PPh_3-CHCP was close to that of using ZnTPP (0.67 h^{-1}),[50] but lower than that of using *fac*-[Ir(ppy)$_3$] (2.30 h^{-1}).[10] The SEC (size exclusion chromatography) curves of PMA obtained in the kinetics study showed a unimodal distribution of MW shifting with the exposure time (Fig. 2c).

Temporal control over polymerization was investigated by intermittently switching off/on the light (Fig. 2d, e). As expected, switching off lights completely ceased the polymerization. The dark period was prolonged up to 12 hours, and a negligible monomer conversion was observed, suggesting that active radicals were not efficiently generated under dark conditions (Fig. S13†). Switching back on the light source resumed the linear chain propagation, as suggested by the agreement between the theoretical and experimental molecular weights (M_n = 16600, $M_{n,th}$ = 16200) and low dispersity ($Đ$ = 1.08) of the resulting polymers (Fig. S14†).

The capability to synthesize block copolymers was also investigated. Results from *in situ* chain extension experiments revealed the high living nature of the resulting polymers. For instance, a PMA macroinitiator (conversion 96%, M_n = 16600, $Đ$ = 1.08) was employed to initiate the second monomer (MEA), which resulted in 93% conversion and offered a well-defined di-

View Article Online DOI: 10.1039/D5SC04010H

block copolymer (M_n = 41700, $Đ$ = 1.11, Fig. 2f). In accordance with the aforementioned experimental procedures, both the ABAB quadri-block copolymer (PMA-*b*-PMEA-*b*-PMA-*b*-PMEA) and the ABC tri-block copolymer (PMA-*b*-PMEA-*b*-Pn-BA) were successfully synthesized (Fig. S15†). Meanwhile, ^{1}H NMR analysis was applied to evaluated the chain-end fidelity of the obtained PMA (M_n = 8800, $Đ$ = 1.06). The ratio of integral value between methine group and methyl group from chain transfer agent was 0.82:3, which was close to the theoretical ratio (1:3) (Fig. S16a†). Furthermore, we performed ultraviolet/visible (UV/Vis) analysis on the synthesized PMA. The absorption peak at λ = 443 nm for the PMA chain end closely matches that of the pristine BTPA RAFT agent, confirming high retention of the RAFT end-group functionality under our experimental conditions (Fig. S16b†).

Table 1. PPh_3-CHCP catalyzed PET-RAFT polymerizations

entry	monomer	PPh_3-CHCP (mg/mL)	[M]/[CTA]	solvent	time (h)	conv. (%)	$M_{n,th}$	M_n	$Đ$
1	MA	2	50:1	DMSO	9	97	4400	4500	1.08
2	MA	2	100:1	DMSO	9	97	8600	8400	1.08
3	MA	2	200:1	DMSO	9	97	16900	17000	1.07
4	MA	2	400:1	DMSO	8	92	31900	35000	1.10
5	MA	2	1000:1	DMSO	6	90	77700	75800	1.17
6[a]	MA	1	1500:1	DMSO	12	91	117700	105200	1.16
7[a]	MA	0.75	2000:1	DMSO	12	85	146600	143800	1.17
8	MEA	2	200:1	DMSO	20	96	25200	25700	1.12
9	BzA	2	200:1	DMSO	20	98	31900	29400	1.10
10	n-BA	2	200:1	DMSO	11	90	22900	24200	1.06
11	TFEA	2	200:1	DMSO	20	92	28400	26600	1.06
12	MMA	0.5	200:1	DMSO	40	90	18200	19500	1.17
13	St	2	100:1	IPA	48	91	9700	10500	1.13
14	OEGMA	2	100:1	Water	6	90	27200	26900	1.13
15	NIPAM	2	200:1	Water	24	80	18300	18100	1.08
16	DMA	2	200:1	Water	8	95	19100	21800	1.13
17	VAc	2	200:1	DMSO	24	50	8800	8000	1.14

Polymerizations were performed under blue light irradiation (2 mW/cm^2) at room temperature without specific statement. Reaction conditions: Entry 1-7, [MA]/[BTPA] = 50, 100, 200, 400, 1000, 1500, 2000/1 in 50 vol% DMSO. Entry 8-11, [M]/[BTPA] = 200/1 in 50 vol% DMSO. [MMA]/[CPADB] = 200/1 in 50 vol% DMSO. [St]/[BTPA] = 100/1 in 50 vol% IPA. Polymerization of styrene was conducted at 40°C. [OEGMA]/[CPADB] = 100/1 in 75 vol% Water. [NIPAM]/[CPADB] = 200/1 in 75 vol% Water. [DMA]/[BTPA]= 200/1 in 50 vol% water. [VAc]/[XAN] = 200/1 in 50 vol% DMSO. DMSO (dimethyl sulfoxide), IPA (isopropanol). [a]1 mW/cm^2 blue light irradiation.

The scope of PPh_3-CHCP catalyzed PET-RAFT could be extended to a variety of monomers. In all cases, well-defined polymers with low dispersity ($Đ$ <1.17) and high monomer conversions were obtained (Table 1 and Fig. S17†). When styrene (a typical low k_p monomer) was applied, 91% conversion and polymers with a dispersity of 1.13 could still be achieved (Table 1, entry 13). Water soluble monomer including OEGMA, NIPAM and DMA were also polymerized in water, achieving monomer conversion of 90%, 80%, and 95%, with dispersity of 1.13, 1.08, and 1.13 of the produced polymers respectively. Polymerization of unconjugated monomers such as vinyl acetate (VAc) was also conducted and achieved 50% monomer conversion (designed DP:200) with relatively low dispersity (1.14) in 24h (Table 1, entry 17), indicating that PPh_3-CHCP-catalyzed PET-RAFT polymerizations was also applicable for low activity monomer. This system also enabled synthesis of polymers with varying degree of polymerization (DP) (targeted from 50 to 2000) (Table 1 and Fig. S18†). For example, PMA with DP of 2000 and a dispersity of 1.17 could be easily obtained with a conversion at 85% within 6 hours. A further increase in the monomer conversion to 92% would result in the broader dispersity of 1.25 (Fig. S19†), which might be attributed to the low diffusion of heterogenous photocatalyst in highly viscous reaction mixture (especially at high monomer conversion) resulting in reduced deactivation process. These results suggested the high flexibility of PPh_3-CHCP catalyzed PET-RAFT polymerization.

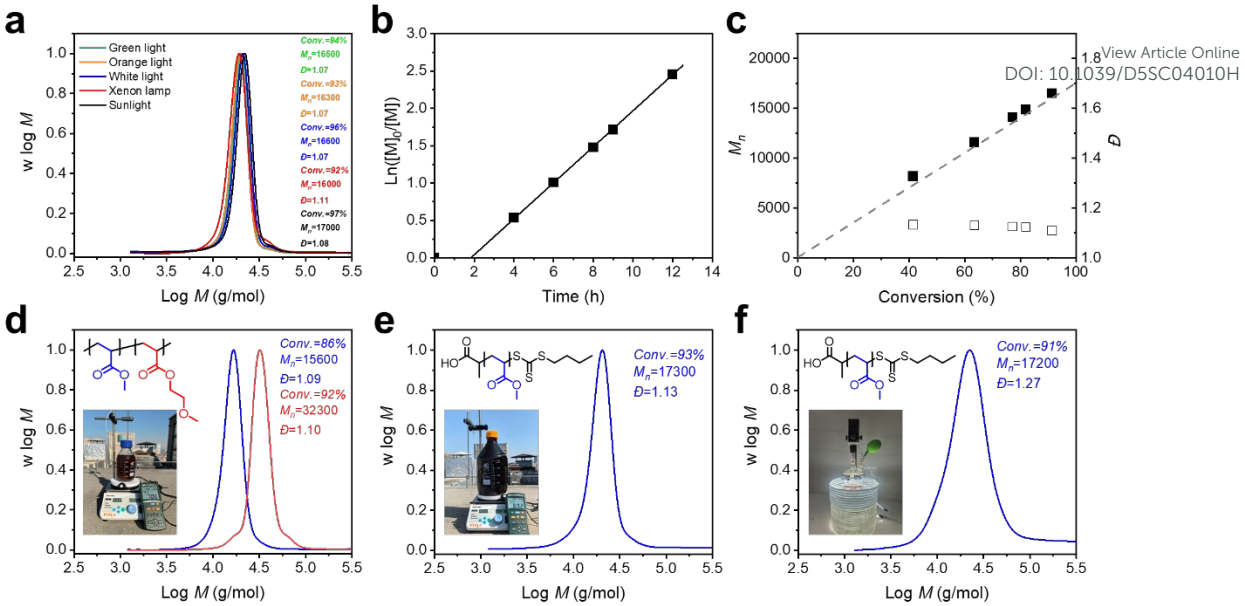

Fig. 3 PET-RAFT polymerizations under broadband lights and sunlight irradiation. (a) SEC traces of PMA synthesized using PPh_3-CHCP as a photocatalyst under green, orange, white, xenon lamp and sunlight irradiation. (b) Kinetics and (c) evolution of molecular weight (M_n, filled points) and dispersity ($Đ$, empty points) in PET-RAFT polymerization under xenon lamp (80 mW/cm²). (d) SEC traces of 250 mL scale of PMA macroinitiator (in blue) and 500 mL scale of PMA_{200}-*b*-$PMEA_{136}$ block copolymer (in red) were synthesized using PPh_3-CHCP under sunlight irradiation. (e) SEC trace of 2 L scale of synthesized using PPh_3-CHCP under sunlight irradiation. (f) SEC trace of 6 L scale of PMA synthesized using PPh_3-CHCP under white light irradiation. Reaction conditions: [M]/[BTPA]= 200/1 in 50 vol% DMSO. PPh_3-CHCP = 2 mg/mL.

PET-RAFT under sunlight irradiation and large-scale production

As PPh_3-CHCP exhibited strong absorption under broadband light irradiation, PPh_3-CHCP catalzyed PET-RAFT polymerization could be extended to green (λ_{max} = 525 nm, 2 mW/cm²), orange (λ_{max} = 590 nm, 2 mW/cm²), and white light (2 mW/cm²) irradiation. All polymerizations achieved ≥ 93% monomer conversion and yield polymers with a low dispersity of 1.07 (Fig. 3a and Table S2†). We need to point out that the reaction time was relatively longer than the blue light. This might be due to the weaker absorption of PPh_3-CHCP in green, orange and white light regions.

More importantly, the wide absorption of PPh_3-CHCP was beneficial to utilize the solar spectrum directly, which covers wavelengths from 250-2500nm. We applied xenon lamp to simulate sunlight, and the reaction kinetic were shown in Fig. 3b, c. A linear dependence of $\ln([M]_0/[M]_t)$ with the exposure time and the experimental molecular weight (MW) values increased linearly with monomer conversion (Fig. S20†). Subsequently, various monomers were applied to evaluate the compatibility of PPh_3-CHCP-catalyzed PET-RAFT system under sunlight irradiation (variation of solar radiation and reported temperature were supplied in and Fig. S21†). Polymerizations of MA, MEA, BzA, n-BA and MMA were successfully performed, resulting in monomer conversions of 97%, 97%, 98%, 91%, and 80% within 8 hours respectively (Table S3 and Fig. S22†). The M_n of obtained polymers were close to their theoretical values, and low dispersity (1.08, 1.10, 1.10, 1.14 and 1.19, respectively) was obtained. The monomer conversion was relatively low for MMA, which may be due to its low activity. These results strongly suggested that PET-RAFT polymerizations could be successfully performed under sunlight irradiation in presence of PPh_3-CHCP. Polymerization was also performed without the photocatalyst under sunlight irradiation, as the UV light and blue light in solar spectrum might trigger photoiniferter RAFT type polymerization. Negligible conversion of MA was observed under xenon lamps, while ~43% conversion achieved under sunlight irradiation (Table S4†), indicating that high-energy photons in the sunlight might trigger the fast photoiniferter initiation process at high ambient temperature and boost PET-RAFT polymerization.

Then, large-scale PPh_3-CHCP catalyzed PET-RAFT polymerization was performed under sunlight. For instance, after 8 hours of sunlight irradiation, a 500 mL scale of polymerization mixture (comprising 250 mL of MA and 250 mL of DMSO) offered 86% monomer conversion, yielding PMA with a dispersity of 1.09 (Fig. 3d). In addition, block copolymer could also be prepared at large scale. A 250 mL of MEA solution (V_{MEA}/V_{DMSO} = 1/1) was *in situ* fed into a 500 mL vial containing 250 mL of prepared PMA macroinitiator solution from sunlight irradiation. After 8 hours of blue light irradiation, well-defined di-block copolymer PMA-*b*-PMEA (M_n = 32300, $Đ$ = 1.10) was obtained (conversion: 92%). There was no obvious difference of molecular weight and dispersity of prepared polymers between the large system and the small vial, and this suggested the robustness and reproducibility of this development.

To further investigate the scalability of the PPh_3-CHCP catalyzed PET-RAFT polymerization system, 2 L scale of MA (V_{MA}/V_{DMSO} = 1/1) was performed under sunlight irradiation (24 h), yielded PMA with a dispersity of 1.13 (conversion 93%, M_n = 17300) (Fig. 3e). Scaled up PET-RAFT polymerization under continuous light irradiation was also evaluated, and reached 91% monomer conversion after 48 h white light irradiation at 6 L

View Article Online
DOI: 10.1039/D5SC04010H

scale (Fig. 3f). To the best of our knowledge, these are the largest PET-RAFT polymerizations using sunlight and white light up to present. The successful large-scale synthesis of both homopolymers and block copolymers demonstrates its great industrial application potential.

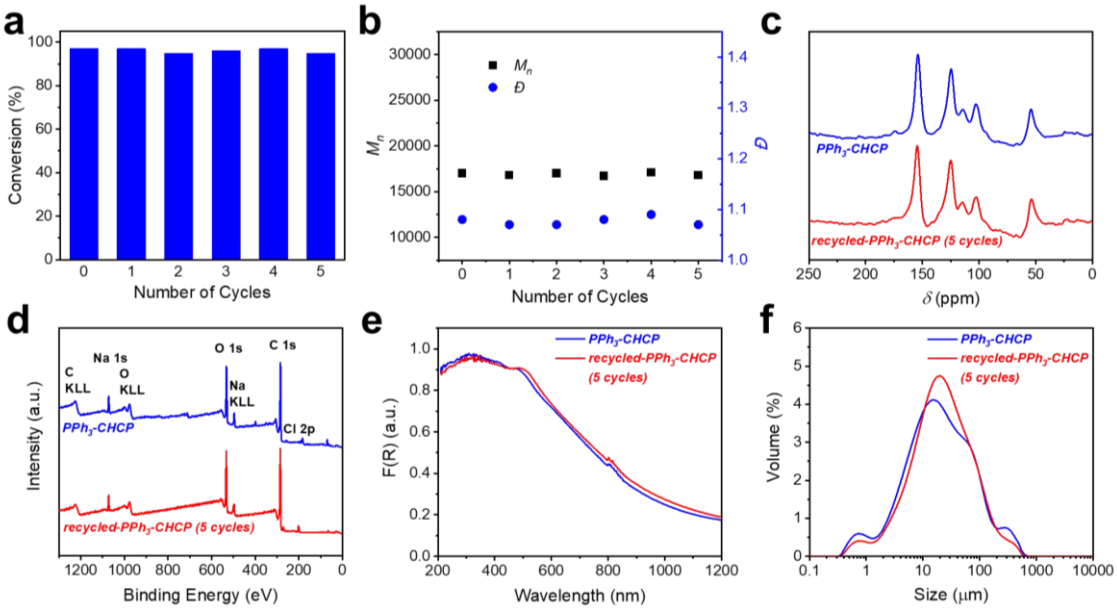

Fig. 4 Results for recycled PPh_3-CHCP photocatalyst after multiple cycles. (a) Monomer conversion and (b) molecular weight (M_n, squares) and dispersity ($Đ$, circles) of the resulting polymers in recycling experiments. (c) Solid-state CP/MAS ^{13}C NMR spectrum (d) Relative XPS survey spectra (e) Solid UV-vis diffuse reflectance and (f) size distribution of PPh_3-CHCP before and after recycling experiments (5 cycles). Reaction conditions: [MA]/[BTPA] = 200/1 in 50 vol % DMSO under blue light irradiation (2 mW/cm^2), PPh_3-CHCP = 2 mg/mL.

Reusability and proposed mechanisms

As a heterogenous catalyst, PPh_3-CHCP could be easily separated from the reaction mixture and reused in multiple polymerization cycles while retaining its high photocatalytic efficiency. After 5 cycles, near quantitative monomer conversions were still obtained, offering polymers with well-controlled molecular weights and low dispersity values (Fig. 4a, b). We also performed gravimetric analysis of PPh_3-CHCP after each recycling cycle. The results indicate an average catalyst recovery yield of ~90% per cycle (corresponding to ~10% mass loss) (Fig. S23†), attributed to unavoidable mechanical losses during recycling process. As normal photocatalyst usually decomposed under long time light irradiation, herein, the photostability of recycled PPh_3-CHCP was further evaluated and the related results were shown in Fig. 4c-f and Fig. S24-25† respectively. No changes in structure, photophysical performance, morphology and size distribution were observed, which demonstrated the good stability under low intensity photocatalytic reaction without using electron donor. Furthermore, we compared the polymerization kinetics using photocatalyst before and after 5 recycle experiments. The $k_{p,app}$ for polymerization of MA using 5 recycled PPh_3-CHCP (0.21 h^{-1}) was similar with initial PPh_3-CHCP under xenon lamp irradiation (0.24 h^{-1}), indicating the high retention of photocatalytic activity after recycling process (Fig. S26†).

As a highly efficient PET-RAFT system, we proposed the oxidative quenching mechanism to elucidate the PPh_3-CHCP catalyzed PET-RAFT polymerization (Fig. 1b). The photo charge transfer reaction occurred between CTA and the excited PPh_3-CHCP under light irradiation, generated initiating radicals and oxidized PPh_3-CHCP (PPh_3-CHCP$^{\bullet+}$). This was supported by fluorescence quenching study on the electron transfer between PPh_3-CHCP and RAFT agent (Fig. S27†), where a continuous decrease in emission intensity was observed on increasing concentration of the RAFT agent. The initiating radicals could either participate in the addition of vinyl monomer or regenerate the PPh_3-CHCP while being deactivated.

Conclusions

In summary, phosphine based crosslinked polymer (PPh_3-CHCP) was exploited as versatile and recyclable photocatalyst for PET-RAFT polymerization of various monomers under broadband light and sunlight irradiation. Polymers with precisely controlled molecular weight properties and high monomer conversions were achieved under varying light irradiation. PPh_3-CHCP were easily separated and reused in following polymerizations without decrease in photocatalytic efficiency. The PPh_3-CHCP enabled successful sunlight-driven polymerization reactions at 2 L, and white light driven polymerization at 6 L, which were the largest scale of sunlight-driven and white light-driven PET-RAFT polymerization reported to date. We anticipated that this PPh_3-CHCP platform will provide a feasible solution for the large-scale PET-RAFT production, highlighting great potential for industrial applications.

Author contributions

T. H., Z. H. F., and W. W. F. conceived the study. Z. H. F. performed the synthesis and characterizations. Y. X. L. carried out the electrochemical measurements. Z. H. X., J. K. Y., X. Y. H., X. Z. W., and X. N. T. discussed the results. W. W. F., L. X., L. X. T., and T. H. supervised the project, acquired funding for this research, and together with Z. H. F. wrote the manuscript.

Conflicts of interest

There are no conflicts to declare.

Data availability

All the data supporting this article have been included in the main text and the ESI. Dataset. https://doi.org/10.6084/m9.figshare.29675291

Acknowledgements

We gratefully acknowledge financial support from the National Natural Science Foundation of China (22171067, 22101275), Postdoctoral Fellowship Program of CPSF (No. GZC20240536), and the Fundamental Research Funds for the Central Universities of China (No.PA2023GDSK0074, No.PA2025GDSK0080).

References

1 N. P. Truong, G. R. Jones, K. G. E. Bradford, D. Konkolewicz, A. Anastasaki, *Nat. Rev. Chem.* 2021, **5**, 859-869.
2 N. Corrigan, K. Jung, G. Moad, C. J. Hawker, K. Matyjaszewski, C. Boyer, *Prog. Polym. Sci.* 2020, **111**, 101311.
3 Y. Lee, C. Boyer, M. S. Kwon, *Nat. Rev. Mater.* 2021, **7**, 74-75.
4 C. Aydogan, G. Yilmaz, A. Shegiwal, D. M. Haddleton, Y. Yagci, *Angew. Chem. Int. Ed.* 2022, **61**, e202117377.
5 D. A. Corbin, G. M. Miyake, *Chem. Rev.* 2021, **122**, 1830-1874.
6 H. Zhou, L. Zhang, P. Wen, Y. Zhou, Y. Zhao, Q. Zhao, Y. Gu, R. Bai, M. Chen, *Angew. Chem. Int. Ed*. 2023, **62**, e202304461.
7 Z. Lu, R. Zhao, H. Yang, X. Fu, Y. Zhao, L. Xiao, L. Hou, *Angew. Chem. Int. Ed.* 2022, **61**, e202208898.
8 J. Sobieski, A. Gorczyński, A. M. Jazani, G. Yilmaz, K. Matyjaszewski, *Angew. Chem. Int. Ed.* 2025, **64**, e202415785.
9 Y. Lee, C. Boyer, M. S. Kwon, *Chem. Soc. Rev.* 2023, **52**, 3035-3097.
10 J. Xu, K. Jung, A. Atme, S. Shanmugam, C. Boyer, *J. Am. Chem. Soc.* 2014, **136**, 5508-5519.
11 C. Wu, N. Corrigan, C. H. Lim, K. Jung, J. Zhu, G. Miyake, J. Xu, C. Boyer, *Macromolecules* 2019, **52**, 236-248.
12 S. A. Logan, Q. Fu, Y. Sun, M. Liu, J. Xie, J. Tang, G. G. Qiao, *Angew. Chem. Int. Ed.* 2020, **59**, 21392-21396.
13 Y. Lee, Y. Kwon, Y. Kim, C. Yu, S. Feng, J. Park, J. Doh, R. Wannemacher, B. Koo, J. Gierschner, M. S. Kwon, *Adv. Mater.* 2022, **34**, 2108446.
14 K. C. Harper, E. G. Moschetta, S. V. Bordawekar, S. J. Wittenberger, *ACS Cent. Sci.* 2019, **5**, 109-115.
15 S. Cañellas, M. Nuño, E. Speckmeier, *Nat. Commun.* 2024, **15**, 307.
16 Y. Zhou, Y. Gu, K. Jiang, M. Chen, *Macromolecules* 2019, **52**, 5611-5617.
17 Z. R. Zhong, Y. N. Chen, Y. Zhou, M. Chen, *Chinese J. Polym. Sci.* 2021, **39**, 1069-1083.
18 Y. Xiao, Z. Xia, W. Hu, B. Liu, C. Lü, *Small* 2024, **20**, 2309893.
19 Z. Xia, B. Liu, Y. Xiao, W. Hu, M. Deng, C. Lü, *ACS Appl. Mater. Interfaces* 2023, **15**, 57119-57133.
20 W. Yao, C. Zhang, X. Wang, Z. Zhang, X. Li, H. Di, *Energy Convers. Manage.* 2018, **164**, 579-587.
21 P. Borah, S. Sreejith, P. Anees, N. V. Menon, Y. J. Kang, A. Ajayaghosh, Y. L. Zhao, *Sci. Adv.* 2015, **1**, e1500390.
22 P. R. Denish, J. A. Fenger, R. Powers, G. T. Sigurdson, L. Grisanti, K. G. Guggenheim, S. Laporte, J. L. Li, T. Kondo, A. Magistrato, M. P. Moloney, M. Riley, M. Rusishvili, N. Ahmadiani, S. Baroni, O. Dangles, M. Giusti, T. M. Collins, J. Didzbalis, K. Yoshida, J. B. Siegel, R. J. Robbins, *Sci. Adv.* 2021, **7**, eabe7871.
23 A. M. Patil, I. S. Nawghare, J. Nithyanandhan, A. V. Ambade, *Macromolecules* 2025, **58**, 2850-2859.
24 G. Lissandrini, D. Zeppilli, F. Lorandi, K. Matyjaszewski, A. A. Isse, L. Orian, M. Fantin, *Angew. Chem. Int. Ed.* 2025, **64**, e202424225.
25 Z. Wu, K. Jung, C. Wu, G. Ng, L. Wang, J. Liu, C. Boyer, *J. Am. Chem. Soc.* 2022, **144**, 995-1005.
26 Q. Wang, F. Y. Bai, Y. Wang, F. Niu, Y. Zhang, Q. Mi, K. Hu, X. Pan, *J. Am. Chem. Soc.* 2022, **144**, 19942-19952.
27 W. Hu, J. Gao, B. Shi, Z. Xia, Y. Xiao, Y. Geng, C. Lü, *ACS Catal.* 2024, **14**, 8148-8159.
28 I. C. Anderson, D. C. Gomez, M. Zhang, S. J. Koehler, C. A. Figg, *Angew. Chem. Int. Ed.* 2025, **64**, e202414431.
29 J. Jiang, G. Ye, F. Lorandi, Z. Liu, Y. Liu, T. Hu, J. Chen, Y. Lu, K. Matyjaszewski, *Angew. Chem. Int. Ed.* 2019, **58**, 12096-12101.
30 M. Chen, J. Hao, W. Zhang, G. Shi, X. Zhang, Z. Cui, P. Fu, M. Liu, X. Qiao, Y. He, X. Pang, *Macromolecules* 2022, **55**, 10788-10796.
31 C. Yu, J. Song, T. I. Kim, Y. Lee, Y. Kwon, J. Kim, J. Park, J. Choi, J. Doh, S. K. Min, S. Cho, M. S. Kwon, *ACS Catal.* 2023, **13**, 665-680.
32 M. Zhang, J. Hao, C. Wang, Y. Zhang, X. Zhang, Z. Cui, P. Fu, M. Liu, G. Shi, X. Qiao, Y. Chang, Y. He, X. Pang, *ACS Catal.* 2024, **14**, 16313-16323.
33 L. Zhang, X. Shi, Z. Zhang, R. P. Kuchel, R. N. Zangeneh, N. Corrigan, K. Jung, K. Liang, C. Boyer, *Angew. Chem. Int. Ed.* 2021, **60**, 5489-5496.
34 L. Zhang, G. Ng, N. K. Kaushik, X. Shi, N. Corrigan, R. Webster, K. Jung, C. Boyer, *Angew. Chem. Int. Ed.* 2021, **60**, 22664-22671.
35 Q. Gao, W. Wang, J. Du, Z. Liu, Y. Geng, X. Ding, Y. Chen, J. Chen, G. Ye, *Angew. Chem. Int. Ed.* 2023, **62**, e202312697.
36 Y. Zhu, D. Zhu, Y. Chen, Q. Yan, C. Y. Liu, K. Ling, Y. Liu, D. Lee, X. Wu, T. P. Senftle, R. Verduzco, *Chem. Sci.* 2021, **12**, 16092-16099.
37 H. Yang, R. Zhao, Z. Lu, L. Xiao, L. Hou, *ACS Catal.* 2023, **13**, 2948-2956.
38 J. Jiang, G. Ye, Z. Wang, Y. Lu, J. Chen, K. Matyjaszewski, *Angew. Chem. Int. Ed.* 2018, **57**, 12037-12042.
39 Y. Yu, S. Tao, Q. Zeng, Z. Ma, K. Zhang, B. Yang, *Carbon Energy* 2025, **7**, e686.
40 X. Luo, Y. Zhai, P. Wang, B. Tian, S. Liu, J. Li, C. Yang, V. Strehmel, S. Li, K. Matyjaszewski, G. Yilmaz, B. Strehmel, Z. Chen, *Angew. Chem. Int. Ed.* 2024, **63**, e202316431.
41 C. Zhao, H. Song, Y. Chen, W. Xiong, M. Hu, Y. Wu, Y. Zhang, L. He, Y. Liu, A. Pan, *ACS Energy Lett.* 2022, **7**, 4389-4397.
42 Z. Xia, B. Shi, W. Zhu, Y. Xiao, C. Lü, *Adv. Funct. Mater.* 2022, **32**, 2207655.
43 S. Shanmugam, S. Xu, N. N. M. Adnan, C. Boyer, *Macromolecules* 2018, **51**, 779-790.
44 Q. Ma, X. Zhang, Y. Jiang, J. Lin, B. Graff, S. Hu, J. Lalevée, S. Liao, *Polym. Chem.* 2022, **13**, 209-219.

View Article Online
DOI: 10.1039/D5SC04010H

45 C. Wu, N. Corrigan, C. H. Lim, W. Liu, G. Miyake, C. Boyer, *Chem. Rev.* 2022, **122**, 5476-5518.
46 M. Zhao, S. Zhu, X. Yang, Y. Wang, X. Zhou and X. Xie, *Macromol. Rapid Commun*. 2022, **43**, 2200173.
47 X. Cao, Z. Lu, H. Yang, R. Zhao, L. Xiao, and L. Hou, *Polym. Chem.* 2024, **15**, 1504-1510.
48 H. Yang, Z. Lu, X. Fu, Q. Li, L. Xiao, Y. Zhao and L. Hou, *Eur. Polym. J.* 2022, **173**, 111306.
49 W. W. Fang, G. Y. Yang, Z. H. Fan, Z. C. Chen, X. L. Hu, Z. Zhan, I. Hussain, Y. Lu, T. He, B. E. Tan, *Nat. Commun.* 2023, **14**, 2891.
50 S. Shanmugam, J. Xu and C. Boyer, *J. Am. Chem. Soc.* 2015, **137**, 9174-9185.

View Article Online
DOI: 10.1039/D5SC04010H

Data availability

All the data supporting this article have been included in the main text and the ESI. Dataset. https://doi.org/10.6084/m9.figshare.29675291